Combined Molecular Mechanics (MM2) and Molecular Orbital (AM1) Study of Periplanone-B and Analogues. Evaluation of Biological Activity from Electronic Properties and Geometries

Kazuko Shimazaki,*[,a] Masataka Mori,[a] Kentaro Okada,[a] Tatsuji Chuman,†[,a] Hitoshi Gotō,[b] Eiji Ōsawa,[b] Kazuhisa Sakakibara[c] and Minoru Hirota[c]

[a] *Life Science Research Laboratory, Japan Tobacco Inc., 6–2 Umegaoka, Midori-ku, Yokohama, Kanagawa 227, Japan*

[b] *Department of Knowledge-Based Information Engineering, Toyohashi University of Technology, 1–1 Hibarigaoka, Tempakucho, Toyohashi 441, Japan*

[c] *Department of Material Engineering, Faculty of Engineering, Yokohama National University, 156 Tokiwadai, Hodogaya-ku, Yokohama, Kanagawa 240, Japan*

Combined molecular mechanics (MM) and semiempirical molecular-orbital (MO) calculations have been applied to the investigation on the conformational and electronic properties of periplanone-B (**1**), a major component of the sex pheromone of American cockroach, and structurally related analogues **2**, **3**, **4** and **5**. In the first step, the geometries of conformers of **1**–**5** were obtained by MM2 combined with a new algorithm for exhaustive generation of ring conformations, CONFLEX2, and an additional set of MM2 force-field parameters. The global minimum (**1A**) of the natural pheromone populates predominantly and is superimposable on the X-ray structure. Minor conformers **1B** and **1C** correspond to the rotamers at the isopropyl group of **1A**. The global minimum of the analogue **2** was identified to have the structure **2A**, which agrees well with the X-ray data. The structural comparison of the stable conformers of the analogues **2**–**5** with **1A** revealed similar ring conformations in the most stable conformers of **2**, **3** and **4**, and the third one of **5**. These results suggest that the ring structure characteristic of the conformer **1A** and the conformer populations must be a significant factor in the biological activity of these analogues. In the next step, the electronic properties were calculated by the semiempirical MO (AM1) method. A significant correlation is found between the biological activity and one of the unoccupied frontier orbitals which is localized around C1–C10–C9 including the carbonyl and spiro-epoxy groups. A newly defined effective frontier parameter: $EF^{(N)}{}_{(s)}$, which regards the orbital electron density, orbital energy, and ring conformation is found to correlate well with the biological activity of these analogues.

The development of computational chemical methods for the treatment of the geometrical and electronic indices of biologically active molecules has provided widely used techniques for the evaluation of structure–activity relationships and for designing new analogues.[1–6] By the use of this new method, we have attempted to investigate the conformational properties of some insect pheromones with verification by conventional NMR and X-ray analyses.[7,8]

Periplanone-B (**1**)[9] is the major sex pheromone component produced by female American cockroach (*Periplaneta americana L.*), and has a unique germacrane structure bearing two epoxy functional groups (Fig. 1). The extremely potent activity (threshold 10^{-13} g),[10] was expected to serve as an effective controlling agent for this insect pest. However, because of the complexity of the structure, known synthetic procedures are not suitable for industrial production of **1**. We have been investigating the conformational and electronic features of periplanone-B and their analogues in order to obtain useful information for the design of new analogues. A structurally simpler analogue (**2**),[11] provided possibilities of creating more useful analogues. Recent conformational analysis of periplanone-B and its analogues by the use of the X-ray crystallographic and NMR methods suggested a conformational resemblance.[12] Following Still's pioneering work,[13] several applications of MM calculations on periplanones have appeared.[14–16] The predicted static structure of **1**[13] was confirmed later by an X-ray crystallographic analysis.[17] It has, however, been pointed out that there were two serious problems on the calculation

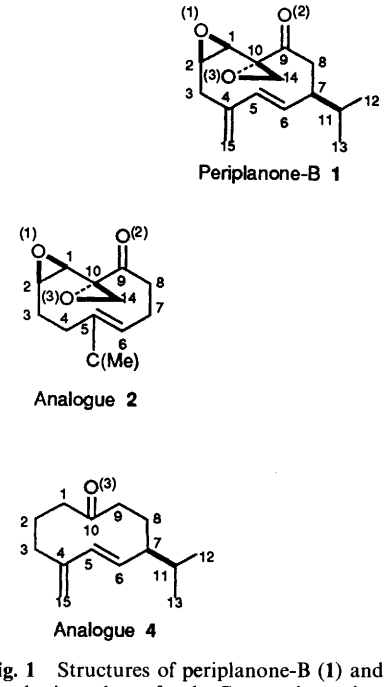

Fig. 1 Structures of periplanone-B (**1**) and analogues **2**–**5**. The same numbering scheme for the C atoms is employed in this paper as has been used for **1** by Persoons *et al.* (1974).[9]

† *Present address:* Head Office, Japan Tobacco Inc., 4–12–62 Higashi-shinagawa, Shinagawa-ku, Tokyo 140, Japan.

Table 1 Fractional non-hydrogen atomic co-ordinates for **2**

Atom	*x*	*y*	*z*
C(1)	0.368 0(2)	0.515 3(3)	0.348 0(1)
C(2)	0.264 4(2)	0.636 1(3)	0.336 5(1)
C(3)	0.136 5(2)	0.573 2(3)	0.296 4(2)
C(4)	0.073 4(2)	0.606 4(3)	0.176 1(2)
C(5)	0.131 3(1)	0.496 1(3)	0.112 5(1)
C(6)	0.126 3(1)	0.308 4(3)	0.111 2(1)
C(7)	0.191 7(2)	0.176 0(3)	0.065 6(1)
C(8)	0.304 9(2)	0.095 7(2)	0.155 3(1)
C(9)	0.376 3(1)	0.258 2(2)	0.219 8(1)
C(10)	0.362 0(1)	0.308 7(2)	0.322 8(1)
C(14)	0.4075(3)	0.1711(2)	0.4096(1)
C(Me)[a]	0.195 6(2)	0.609 7(3)	0.057 7(2)
O(1)	0.344 8(1)	0.569 6(2)	0.439 88(9)
O(2)	0.443 8(1)	0.352 2(2)	0.192 1(1)
O(3)	0.280 7(1)	0.194 3(2)	0.351 49(9)

[a] Methyl group attached to the C(5) position of the ten-membered ring.

Table 2 Bond lengths/Å and angles/° involving the non-hydrogen atoms for **2** (esds in parentheses)

Bond length			
C(1)–C(2)	1.470(3)	C(10)–C(1)	1.500(2)
C(2)–C(3)	1.492(3)	C(5)–C(Me)[a]	1.494(3)
C(3)–C(4)	1.538(3)	C(10)–C(14)	1.468(2)
C(4)–C(5)	1.515(3)	C(1)–O(1)	1.431(2)
C(5)–C(6)	1.332(3)	C(2)–O(1)	1.451(2)
C(6)–C(7)	1.500(3)	C(9)–O(2)	1.214(2)
C(7)–C(8)	1.552(2)	C(10)–O(3)	1.432(2)
C(8)–C(9)	1.504(2)	C(14)–O(3)	1.437(2)
C(9)–C(10)	1.515(2)		
Bond angle			
C(1)–C(2)–C(3)	125.4(2)	C(4)–C(5)–C(Me)[a]	116.2(2)
C(2)–C(3)–C(4)	111.7(2)	C(6)–C(5)–C(Me)[a]	124.2(2)
C(3)–C(4)–C(5)	112.3(2)	O(1)–C(2)–C(3)	118.3(2)
C(4)–C(5)–C(6)	119.6(2)	O(1)–C(2)–C(1)	58.7(1)
C(5)–C(6)–C(7)	127.0(2)	O(1)–C(1)–C(2)	60.0(1)
C(6)–C(7)–C(8)	110.2(1)	O(1)–C(1)–C(10)	116.9(1)
C(7)–C(8)–C(9)	108.4(1)	C(10)–O(3)–C(14)	61.5(2)
C(8)–C(9)–C(10)	118.7(1)	O(3)–C(10)–C(1)	118.0(1)
C(9)–C(10)–C(1)	115.4(1)	O(3)–C(10)–C(9)	116.4(1)
C(10)–C(1)–C(2)	125.3(2)	O(3)–C(10)–C(14)	59.4(1)
C(1)–O(1)–C(2)	61.3(1)	O(3)–C(14)–C(10)	59.1(1)
C(8)–C(9)–O(2)	122.7(1)	C(9)–C(10)–C(14)	116.6(1)
C(10)–C(9)–O(2)	118.6(1)	C(1)–C(10)–C(14)	119.6(2)

[a] Methyl group attached to the C(5) position of the ten-membered ring.

methods, namely, the lack of force-field parameters for the functionalities including the epoxy groups, and the difficulty of generation of possible conformations, since ten-membered ring compounds, such as **1**, normally exist in several local minima with small energy differences. To solve these problems, we have developed the new force-field parameters for the epoxy group,[18] and employed a newly developed program, CONFLEX,[19]* for the exhaustive generation of geometries for ring systems. The conformational analysis of the analogues **4** and **5** by use of CONFLEX2 has been reported.[8]

* CONFLEX2 is based on one of the latest and most effective algorithms, called 'corner flapping', developed for the search of conformational space of cyclic molecules. The program has been carefully tested for a number of cycloalkanes and confirmed, for example, to generate 68 conformers of cycloheptadecane known to exist (in the framework of MM2) within 2 kcal mol^{-1} from its global minimum conformation (H. Gotō and E. Ōsawa, submitted for publication in *Tetrahedron Lett.*). Since we consider throughout this work only those conformers having populations higher than 2%, our search in this range is considered to be complete.

Furthermore, we have pointed out that the oxygen-containing functionalities of the analogues may play an important role in their biological processes, because their activities decreased with removal or substitution of these functionalities.[12] Therefore, the relationship between the electronic effects of these functionalities and the observed activity must be noted.

In this study, we carried out a complete molecular mechanics analysis of periplanone-B and several analogues by CONFLEX/MM2. The electronic properties of the stable conformers were calculated by means of a semiempirical AM1 method. On the basis of these calculated results, we discuss the correlation of some geometrical and electronic indices with the biological activities of the compounds examined.

Method

The preparation and characterization of compounds **1**–**5** have been described previously.[11,12,20] Their biological activities have been assessed by behavioural tests: the threshold dosages for **1**, 10^{-13} g; **2**, 10^{-9} g; **3** 10^{-7} g; **4**, 10^{-6} g; **5**, 10^{-5} g, and the experimental details have also been reported.[10]

Computational Details.—MM2 program, version '87, was obtained from Molecular Design Ltd.[21] and used for geometry optimization. The new force-field parameters for epoxy functional groups were determined by using the results of *ab initio* calculations on model compounds of periplanone-B and the reported structural data of epoxy compounds.[18] All possible geometries of the ring conformations were generated by CONFLEX2 and optimized by MM2.[19] The Boltzmann population of each energy minimum at 25 °C was calculated on the basis of their steric energy.

Average vicinal H–H coupling constants ($^3J_{HH}$) were calculated from 38 energy minima of **1** and 70 of **3** using Altona's empirical modification of the Karplus equation.[22]

The optimized geometries obtained by CONFLEX/MM2 calculations were used as the input data for AM1 (AMPAC version 2.1)[23] calculations for stable conformers, having populations above 1.0%. The total number of the stable conformers calculated are: **1**, 7; **2**, 4; **3**, 6; **4**, 12; **5**, 11. Computations were carried out on an IRIS 4D/320GTX workstation (Silicon Graphics). The three-dimensional structures, the frontier orbital extension and superposition of the target molecules were visualized by the use of the QUANTA program (Polygen Co., USA).

Ultraviolet Spectroscopy.—λ_{max} was evaluated from the population-weighted energy differences between the first excited and the ground state of conformers by taking the configuration interaction (CI) into account.

X-Ray Crystal Structure Analysis of **2**.—A colourless prism crystal of **2** having approximate dimensions 0.50 × 0.20 × 0.30 mm was mounted on a glass fibre at a temperature of −120 ± 1 °C. An experiment at room temperature resulted in sublimation of the crystal. All measurements were made on a Rigaku AFC6R diffractometer with graphite monochromated Mo-Kα radiation and a 12 kW rotating anode generator. The crystallographic data for **2**: $C_{12}H_{16}O_3$, formula weight 206.28, monoclinic, $P2_1/c$ (No. 14); a = 12.014(2), b = 7.086(2), c = 13.586(2) Å, β = 112.151(9)°, V = 1071.3(4) Å^3, Z = 4, D_{calc} = 1.291 g cm^{-3}, $F(000)$ = 448, μ(Mo-Kα) = 0.86 cm^{-1}, r(Mo-Kα) = 0.710 69 Å. The structure of **2** was solved by direct methods using DIRDIF[24] and MITHRIL[25] programs. Non-hydrogen atoms were refined anisotropically. Hydrogen atoms were refined isotropically. The final cycle of full-matrix least-squares refinement was based on 1482 observed reflections [$I >$

Table 3 Conformational properties and X-ray data of **1**

	1A	1B	1C	1D	X-ray[a]
Ring conformation[b]	[1'333']	[1'333']	[1'333']	[1'333']	[123'1'3']
ΔE_s/kcal mol^{-1}	0.0	0.99	1.35	1.69	
Boltzmann dist. (%) at 25 °C	67.90	12.80	7.01	3.95	
Dihedral angle/°					
C(10)–C(1)–C(2)–C(3)	2.4	2.2	2.4	4.7	−1.5
C(1)–C(2)–C(3)–C(4)	−90.1	−91.1	−90.7	−68.3	−90.0
C(2)–C(3)–C(4)–C(5)	74.9	73.2	74.4	20.2	80.0
C(3)–C(4)–C(5)–C(6)	35.1	34.9	33.9	114.6	29.5
C(4)–C(5)–C(6)–C(7)	−167.5	−166.7	−166.6	−169.2	−166.4
C(5)–C(6)–C(7)–C(8)	109.0	113.3	111.6	89.0	110.1
C(6)–C(7)–C(8)–C(9)	−40.4	−43.5	−41.6	−59.7	−40.8
C(7)–C(8)–C(9)–C(10)	92.4	91.1	91.6	87.4	95.6
C(8)–C(9)–C(10)–C(1)	−147.2	−144.2	−145.8	−140.0	−148.9
C(9)–C(10)–C(1)–C(2)	96.4	98.7	97.4	114.9	97.3
C(8)–C(7)–C(11)–H(11)	60.3	−51.6	−177.4	60.4	57.7
C(9)–C(8)–C(7)–C(11)	−163.8	−170.4	−168.2	177.1	−166.4

[a] Data from the X-ray crystallographic analysis of **1**. [b] Modified Dale nomenclature. Primes indicate a pseudo-corner ($g^+ g^-$), ref. 8. 38 Energy minima were obtained from 250 initial geometries which were generated by CONFLEX2.

Table 4 Conformational properties of **2**

	2A	2B	2C	2D	X-ray[a]
Ring conformation[b]	[1'333']	[232'3']	[3'34]	[2323]	[123'1'3']
ΔE_s/kcal mol^{-1}	0.0	1.06	1.15	2.19	
Boltzmann dist. (%) at 25 °C	74.91	12.46	10.76	1.84	
Dihedral angle/°					
C(10)–C(1)–C(2)–C(3)	1.2	−0.2	1.1	−2.5	−0.9
C(1)–C(2)–C(3)–C(4)	−90.3	−88.0	−86.3	−98.9	−93.5
C(2)–C(3)–C(4)–C(5)	56.0	60.8	69.9	46.9	61.6
C(3)–C(4)–C(5)–C(6)	72.4	−85.5	−85.6	60.6	66.2
C(4)–C(5)–C(6)–C(7)	−174.6	172.2	174.7	−168.8	171.1
C(5)–C(6)–C(7)–C(8)	95.2	−107.0	−76.1	73.7	99.7
C(6)–C(7)–C(8)–C(9)	−46.1	68.7	−46.1	66.5	−51.3
C(7)–C(8)–C(9)–C(10)	89.8	−77.5	84.1	−74.4	98.0
C(8)–C(9)–C(10)–C(1)	−142.5	−20.1	−116.7	−41.7	−144.2
C(9)–C(10)–C(1)–C(2)	104.8	118.7	119.5	117.8	103.9

[a] Data from the X-ray crystallographic analysis of **2**. [b] Modified Dale nomenclature. Primes indicate a pseudo-corner ($g^+ g^-$), ref. 8. Nine energy minima were obtained from 60 initial geometries which were generated by CONFLEX2.

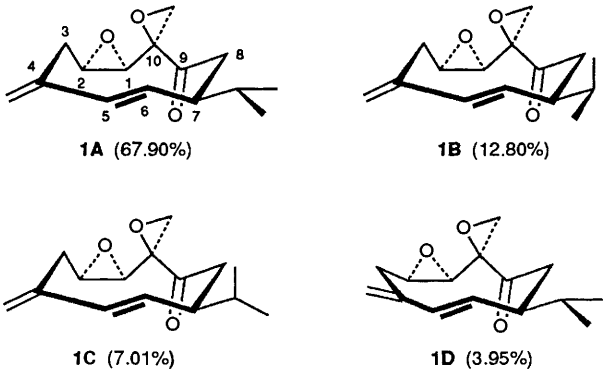

Fig. 2 Major conformers of periplanone-B **1**

$3.00\sigma(I)$] and 201 variable parameters and converged (the largest parameter shift was 0.06 times its esd) with unweighted and weighted agreement factors $R = \Sigma||F_o| - |F_c||/\Sigma|F_o| = 0.034$, $R_w = [(\Sigma w(|F_o| - |F_c|)^2/\Sigma wF_o^2)]^{\frac{1}{2}} = 0.043$.

The standard deviation of an observation of unit weight was 1.81. The weighting scheme was based on counting statistics and included a factor ($p = 0.03$) to downweight the intense reflections. Fractional non-hydrogen atomic coordinates are listed in Table 1, and bond lengths and valence angles of the non-hydrogen atoms in Table 2, respectively. Full lists of bond lengths and bond angles for **2**, together with hydrogen atom coordinates, thermal parameters and tables of least-squares planes, have been deposited at the Cambridge Crystallographic Data Centre.*

Results and Discussion

Molecular-mechanics Calculations.—The conformational properties of major conformers over 2% Boltzmann populations at 25 °C of **1**, **2** and **3** are summarized in Tables 3, 4 and 5, respectively. The results of **4** and **5** have already been reported.[8]

Periplanone-B (**1**). MM analysis on **1** identified four dominant conformers. As can be seen in Fig. 2 and Table 3, the three most stable conformers, (**1A**, **1B**, **1C**), have almost identical twist-

* For details of the CCDC deposition scheme, see 'Instructions for Authors,' *J. Chem. Soc., Perkin Trans. 2*, 1992, issue 1.

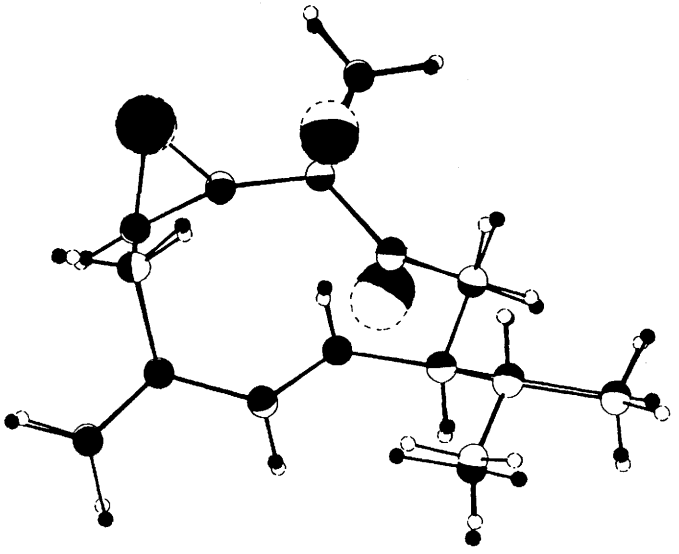

Fig. 3 Superimposition of the global minimum of **1** (**1A**) (filled) and the X-ray structure of **1**

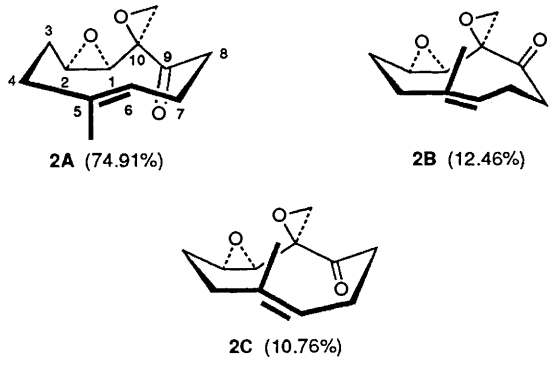

Fig. 4 Major conformers of analogue **2**

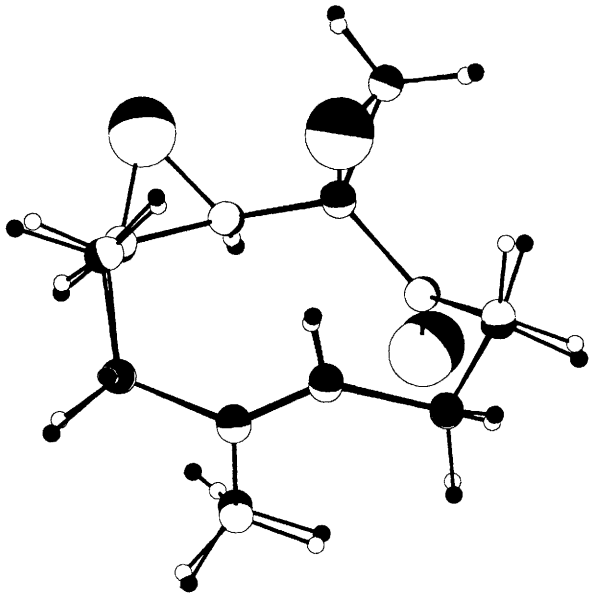

Fig. 5 Superimposition of the global minimum of **2** (**2A**) (filled) and the X-ray structure of **2**

chair (TC) ring conformations; they differ only in the rotation of the isopropyl group. The spiro-epoxy carbon (C10) and the transannular alkenic carbon (C5) are closely located. The combined population of **1A**–**1C** amounts to 88% and in this regard the ten-membered ring of periplanone-B is rather 'rigid'. The calculated ring structure common to these three conformers

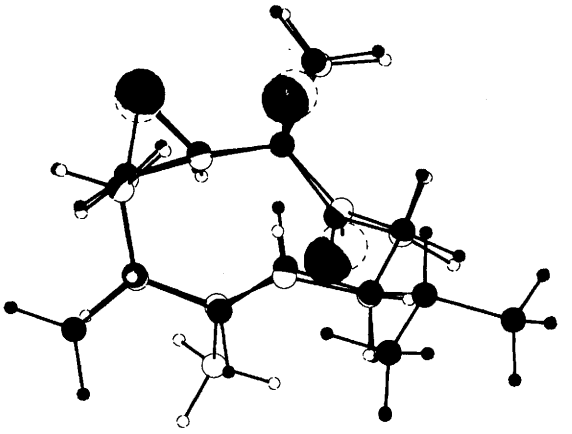

Fig. 6 Superimposition of the global minimum of **2** (**2A**) and of **1** (**1A**) (filled)

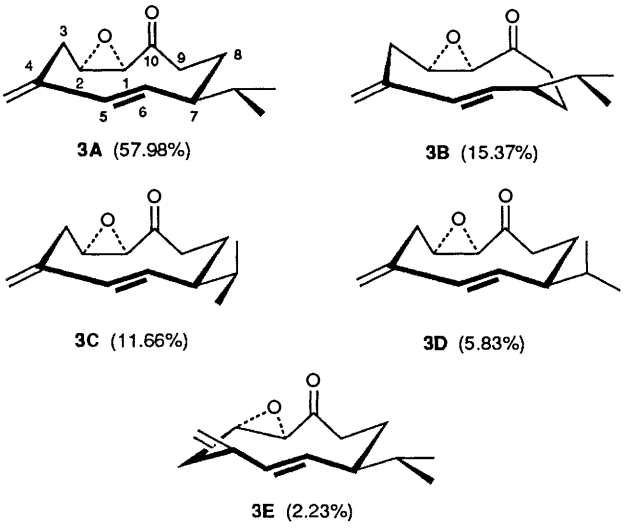

Fig. 7 Major conformers of analogue **3**

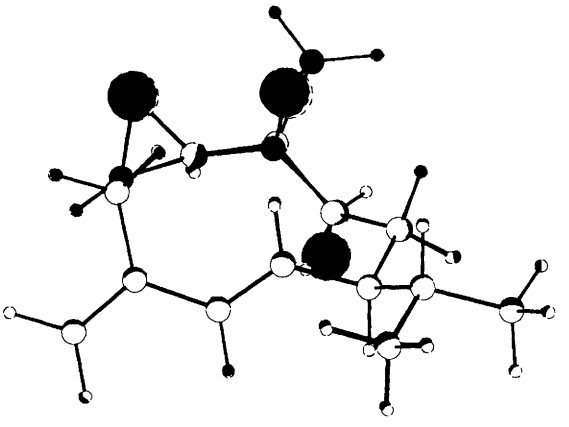

Fig. 8 Superimposition of the global minimum of **3** (**3A**) and of **1** (**1A**) (filled)

(**1A**, **1B** and **1C**) is superimposable on the experimental X-ray structure[17] (Fig. 3). The fourth conformer (**1D**) is given the same ring nomenclature but has slightly different dihedral angles around C1–C2–C3–C4–C5 from those of the major isomers, as the result of flipping in the exomethylene double bond (Table 3). The dihedral angle of C15–C4–C5–C6 in **1D** (= −61.22°) is about 90° different from those of the three major conformers (*ca.* −154°). Except for this point, relative orientation of three oxygen-containing functional groups is uniquely retained among the stable conformers. The oxygen atoms of carbonyl

Table 5 Conformational properties of 3

	3A	3B	3C	3D	3E
Ring conformation[b]	[1′333′]	[2323]	[1′333′]	[1′333′]	[1′3′2′4′]
ΔE_s/kcal mol^{-1}	0.0	0.79	0.95	1.36	1.93
Boltzmann dist. (%) at 25 °C	57.98	15.37	11.66	5.83	2.23
Dihedral angle/°					
C(10)–C(1)–C(2)–C(3)	2.7	−1.3	2.7	2.8	−0.1
C(1)–C(2)–C(3)–C(4)	−88.5	−95.6	−89.5	−89.2	9.8
C(2)–C(3)–C(4)–C(5)	74.2	58.4	72.9	73.6	−68.2
C(3)–C(4)–C(5)–C(6)	34.0	37.9	34.3	33.3	146.4
C(4)–C(5)–C(6)–C(7)	−167.4	−165.5	−166.5	−166.5	−161.3
C(5)–C(6)–C(7)–C(8)	110.0	86.0	113.5	112.7	87.7
C(6)–C(7)–C(8)–C(9)	−41.0	63.7	−44.1	−42.7	−49.4
C(7)–C(8)–C(9)–C(10)	80.5	−64.0	80.5	80.6	76.8
C(8)–C(9)–C(10)–C(1)	−152.7	−62.0	−150.7	−151.4	−162.2
C(9)–C(10)–C(1)–C(2)	111.6	127.7	113.0	112.3	102.7
C(8)–C(7)–C(11)–H(11)	61.1	63.4	−51.3	−177.5	60.8
C(9)–C(8)–C(7)–C(11)	−164.8	−60.5	−171.5	−169.7	−172.8

[a] Modified Dale nomenclature. Primes indicate a pseudo-corner (g^+ g^-), ref. 8. 73 Energy minima were obtained from 527 initial geometries which were generated by CONFLEX2.

Table 6 Comparison of the observed vicinal NMR coupling constants with calculated values for proton on 1 and 3

		J/Hz								
Compound		1–2	2–3α	2–3β	7–8α	7–8β	8α–9α	8β–9α	8α–9β	8β–9β
1	Calc.	7.75	4.83	10.78	5.15	11.48				
	Obs.	4.0	4.0	10.2	5.7	11.0				
3	Calc.	7.59	4.41	10.7	5.05	10.12	1.00	11.32	8.54	0.97
	Obs.	4.0	3.5	10.1	—	11.5	1.1	12.5	6.5	1.2

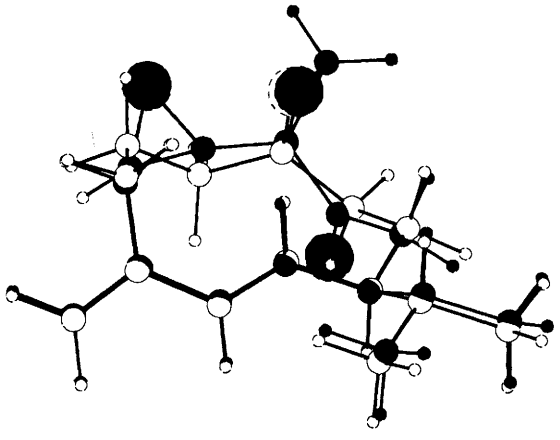

Fig. 9 Superimposition of the global minimum of **4** and of **1** (**1A**) (filled)

[O(2)] and of spiro-epoxy groups [O(3)] are located in the opposite sides of ring plane (dihedral angle = −179°). The dihedral angle O(1)–C1–C10–O(3) (= 19°) shows that the two oxygen atoms of the epoxy groups are spatially close. The calculated vicinal H–H coupling constants ($^3J_{HH}$) essentially agree with those observed, except that of the strained epoxy protons (Table 6).

Analogue **2**. In contrast with the case of **1**, the three major conformers have rather different structural features from each other (Fig. 4 and Table 4). Superpositioning clearly showed good overlap of the most stable conformer **2A** with the X-ray structure (Fig. 5). The conformer **2A** with 74.91% population has a ring conformation very similar to that of **1A** as shown in Fig. 6. Hence it is shown that the removal of isopropyl and exomethylene groups from **1** does not change on the ring conformational behaviour, as far as the global energy-minimum structure is concerned. The ring conformations of other conformers are significantly different. However, the relative orientations of the two epoxy rings in **2B** and **2C** are still conserved as in the best conformer, although the carbonyl and methyl groups in these conformers are flipped.

Analogue **3**. The CONFLEX/MM analysis identified five stable conformers for **3**, which are shown in Fig. 7 and Table 5. The most stable (**3A**), the third (**3C**) and the fourth (**3D**) conformers have the same ring structure as **1A**. The combined population of these three isomers amounts to 75%. Fig. 8 shows a superposition of **3A** with **1A**. Again, the relative orientation of oxygen atoms is maintained as found in the case of periplanone-B. Judging from a comparison of dihedral angles along the C7–C8–C9–C10–C1 region of the ring in **3A** with those in **1A**, it should be pointed out that the oxygen atom [O(3)] of the spiro-epoxy group in **1A** and the carbonyl oxygen atom in **3A** are located at essentially the same positions relative to the ring planes. As shown in Table 6, the calculated vicinal H–H coupling constants ($^3J_{HH}$) agree with the observed values, except those of the strained epoxy protons.

Analogue **4** *and germacrene-D* (**5**). As reported in our previous paper,[11] the global minimum of **4** and the third conformer of **5** were found to be superimposable on **1A** (Figs. 9 and 10).

CONFLEX/MM2 calculations revealed that the global minimum conformation of the natural pheromone (**1A**) overlapped well with those of **2**, **3** and **4**, and the third most stable conformation of **5**. One attractive hypothesis would be to assume that activity of a periplanone-B analogue is related to the total population of the conformers having the ring conformation superimposable on that of the global minimum of **1**. CONFLEX/MM2 study suggests that the ring conformation of **1A** is the biologically important structure.

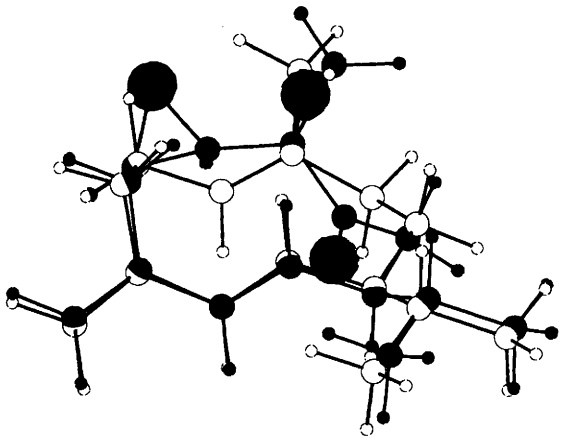

Fig. 10 Superimposition of the third conformer of **5** and the global minimum of **1** (**1A**) (filled)

Molecular-orbital Calculations.—Several studies, which have attempted to correlate the electronic structure, especially frontier orbitals, with biological activity, have been reported.[2–4] Ramos and Neto[3] reported least-squares fits that show a correlation between hypolipidemic activity and LUMO energy and carbonyl polarities in phthalimide and related compounds. Recently, we have highlighted an important role of the oxygen-containing functionalities of the analogues in biological processes.[1,2] Thus, in order to investigate the correlation between the electronic properties and their pheromone activity, an AM1 study was carried out on the stable conformers of the compounds **1** to **5** obtained by CONFLEX/MM2. In Figs. 11, 12 and 13, are reproduced the frontier-orbital extensions and the frontier orbital energy (eV) of the most stable conformers of **1**, **2** and **3**, respectively.

Periplanone-B (**1**). Both the highest occupied molecular orbital (HOMO) and the lowest unoccupied molecular orbital (LUMO) of **1A** are localized mainly at the conjugated-diene (C15–C4–C5–C6) moiety (Fig. 11). It is noteworthy that the orbital energy of the next-LUMO is only 0.12 eV higher than that of the LUMO. The next-LUMO is localized around the carbonyl and adjacent spiro-epoxy groups. The frontier electron density of the next-LUMO is particularly concentrated at the carbonyl carbon atom, but relatively low at the *endo*-epoxy group. The same feature of the frontier orbitals is also found in the second (**1B**) and the third (**1C**) stable conformers. In the fourth conformer (**1D**), whose ring structure is slightly different from those of the three most stable conformers as the result of flipping of exomethylene group, the LUMO is localized at the carbonyl and spiro-epoxy moiety, and the next-LUMO exists at the conjugated diene moiety (C15–C4–C5–C6).

Analogue **2**. As shown in Fig. 12, the HOMO and next-LUMO of the most stable conformer of **2** are localized around the double-bond moiety at C5–C6. In this case, LUMO is localized at the carbonyl and spiro-epoxy moiety, whose extension resembles that of the next-LUMO of **1A**. The orbital-energy gap between the LUMO and next-LUMO is larger than that found in **1A**. In other conformers of **2**, the features of the frontier orbitals are essentially the same as those in the most stable conformer.

Analogue **3**. In Fig. 13, it can be seen that the HOMO and LUMO of the global minimum of **3** are distributed around the diene moiety as are those of **1A**. The next-LUMO is localized mainly around the carbonyl functional group [C(10)–O(3)]. The energy difference between the two unoccupied frontier orbitals is about 0.4 eV in the global minimum of **3**.

Analogue **4**. In all stable conformers of **4**, the extension of the HOMO and LUMO essentially resembles that of the global minimum of **3**. The frontier electron density of the next-LUMO is concentrated at the carbonyl carbon atom. A rather large energy difference (0.73 eV) between the two unoccupied frontier orbitals (LUMO; 0.441 eV; next-LUMO; 1.171 eV) is found in the global minimum of **4**.

Germacrene-D **5**. In all stable conformers of **5**, the extension of the HOMO and LUMO is similar to that of **1A**. The next-LUMO is localized at the double bond [C(10)–C(1)].

The distribution of the LUMO and next-LUMO on the ten-membered ring systems in compounds **1**–**5**, can be classified into two groups. In the first group, unoccupied frontier orbitals are localized mainly at the C9–C10–C1 region of the ten-membered ring, extending to the carbonyl and spiro-epoxy groups of **1**, **2**, **3** and **4**, and to the double bond of **5**. In the second group, they are localized at the C15–C4–C5–C6 region of the ten-membered ring, which covers the diene part of **1**, **3**, **4** and **5**, and the double bond of **2**. As the former unoccupied frontier orbital is localized around the 'upper' part of ten-membered ring in the structural formula, we call it the frontier unoccupied orbital around upper part of ten-membered ring (abbreviated as $FUMO_{upper}$). In the same manner, the latter unoccupied frontier orbital is called the frontier unoccupied orbital around lower part of ten-membered ring (abbreviated as $FUMO_{lower}$).

Theoretical Aspects.—In order to take into account the contribution of every stable conformer whose Boltzmann population is larger than 1% at 25 °C, the total energy and orbital energy are both population-weighted for the discussion. The reliability of the AM1 calculations on periplanone-B (**1**) and its analogues was confirmed by comparison of the calculated (λ = 224.4 nm) and observed (λ = 225.4 nm) λ_{max} value of **1**. The population-weighted frontier-orbital energies of HOMO, $FUMO_{lower}$ and $FUMO_{upper}$ of **1**–**5** are shown in Table 7. In general, the population-weighted orbital energy of $FUMO_{lower}$ (localized at the diene moiety) is lower than that of $FUMO_{upper}$ (localized at the spiro-epoxy and carbonyl groups) except for the case of **2**. The small energy gap between $FUMO_{lower}$ and $FUMO_{upper}$ of **1** is noteworthy. Of the frontier orbitals, only the population-weighted energy of $FUMO_{upper}$ shows good correlation with the biological activity (R = 0.849, Fig. 14), although those of HOMO and $FUMO_{lower}$ do not show a linear relationship.

Effective Frontier Parameter [$EF^{(N)}{}_{(s)}$].—Since the MM study indicated that the ring conformation is important for biological activity of periplanone analogues, the correlation between biological activity and electronic indices was further examined with respect to the structural factor. We derive the 'effective frontier parameter' [$EF^{(N)}{}_{(s)}$] as a biological activity index in order to incorporate the contribution of the proper structure of stable conformers into electronic properties. The parameters were determined from the frontier electron density on all carbon and oxygen atoms, which constitute the ten-membered ring or any functional groups except the isopropyl group, and the orbital energy in $FUMO_{upper}$ of the stable conformers and their population. Conformers whose population at 25 °C is above 1.0% were taken into account for the calculation of the 'effective frontier parameter'. It is defined as shown in eqns. (1)–(3)

$$f_r^{(N)} = 2C^2{}_{r(FUMO_{upper})} \quad (1)$$

$$Ef_r^{(N)} = \Sigma\{f_r^{(N)}{}_\mu / E_{(FUMO_{upper})\mu}\} \times Pop_\mu \quad \mu = 1\text{–}M \quad (2)$$

$$EF^{(N)} = \Sigma\{Ef_r^{(N)}\} \quad r = 1\text{–}R \quad (3)$$

where $f_{(r)}{}^{(N)}$ is the frontier electron density in $FUMO_{upper}$ of atom r, r is the atom number (excepting protons), R is the total

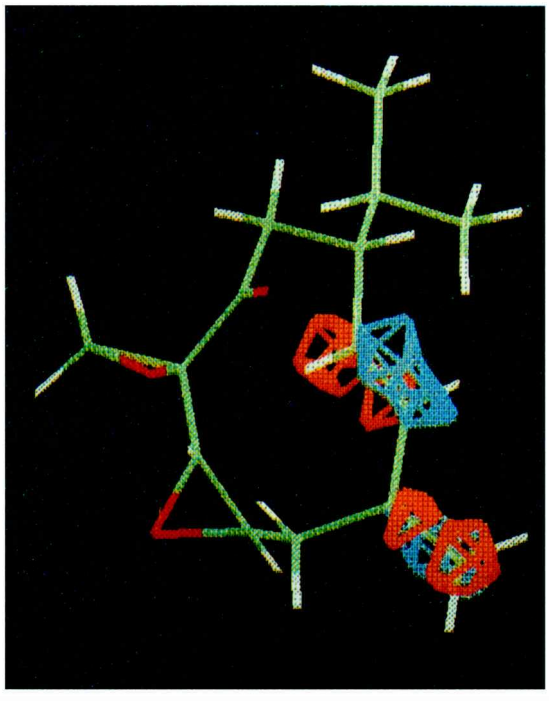

HOMO (E = −9.286)

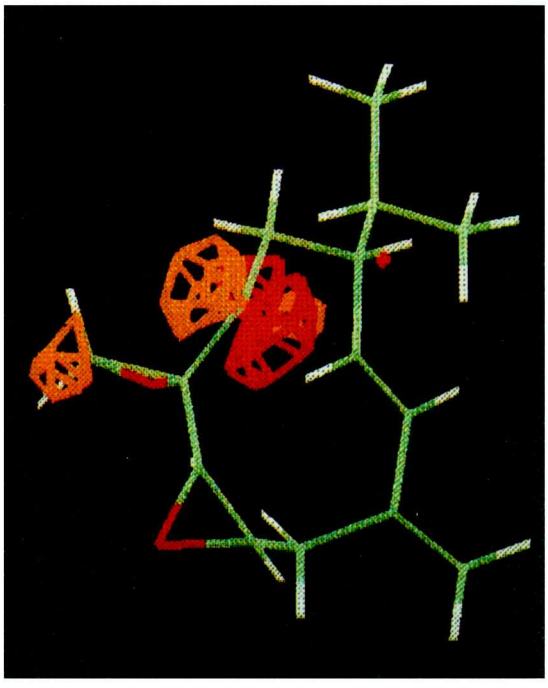

next-LUMO (E = 0.477)

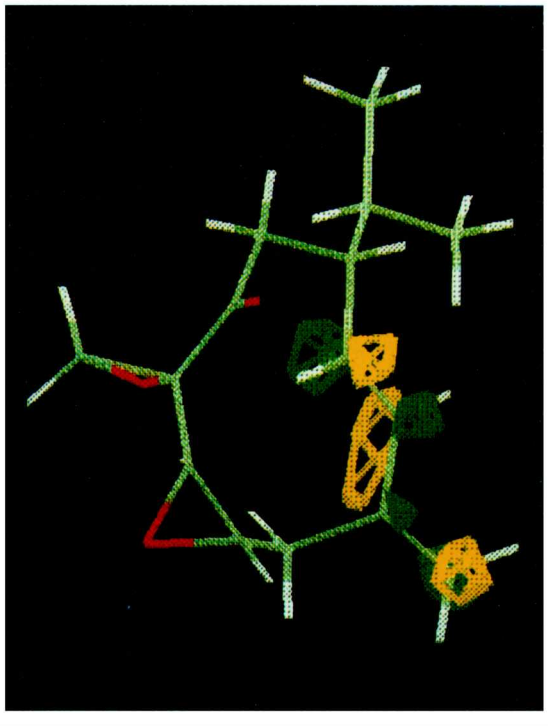

LUMO (E = 0.360)

Fig. 11 Frontier orbital of the global minimum of **1**; the value of each frontier-orbital energy (E/eV) is shown in parentheses

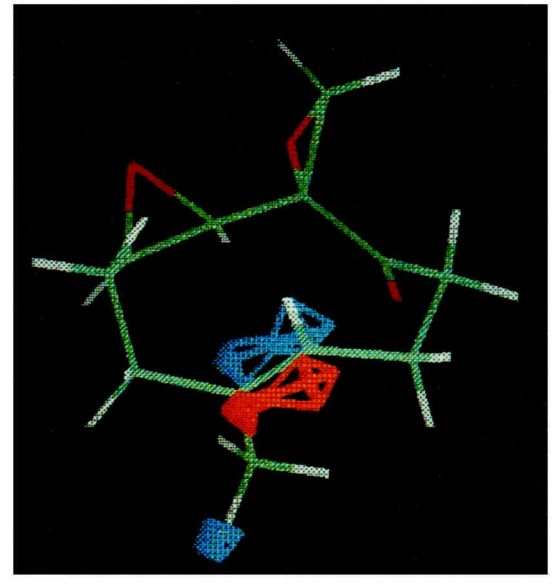

HOMO (E = −9.562)

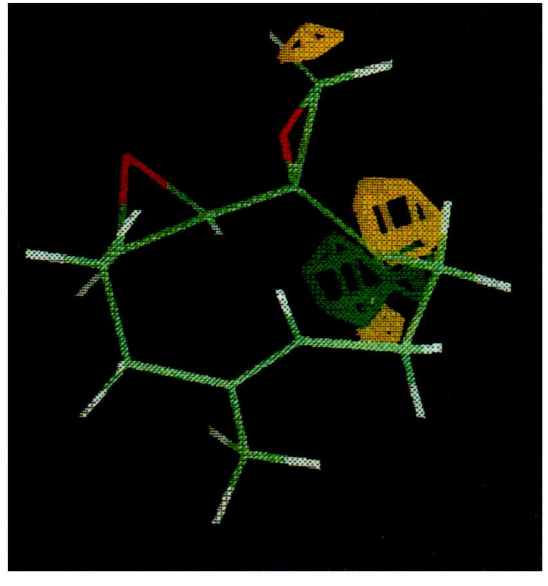

LUMO (E = 0.511)

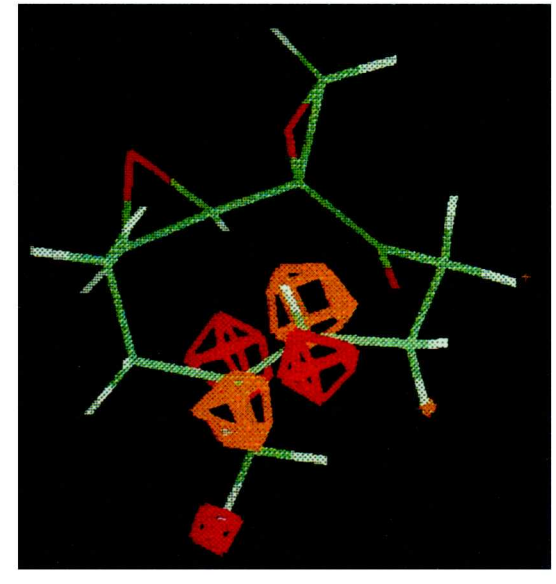

next-LUMO (E = 1.027)

Fig. 12 Frontier orbital of the global minimum of **2**; the value of each frontier orbital energy (E/eV) is shown in parentheses

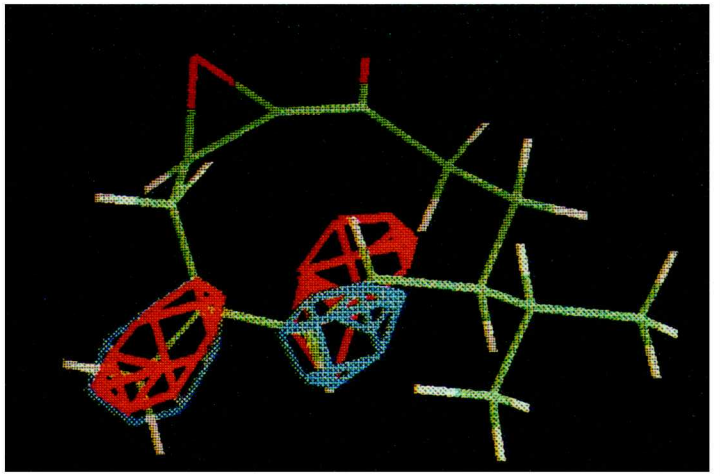

HOMO (E = −9.324)

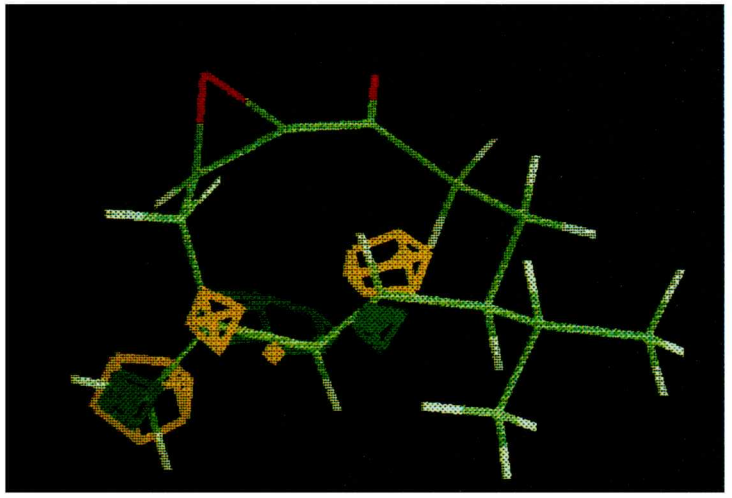

LUMO (E = 0.289)

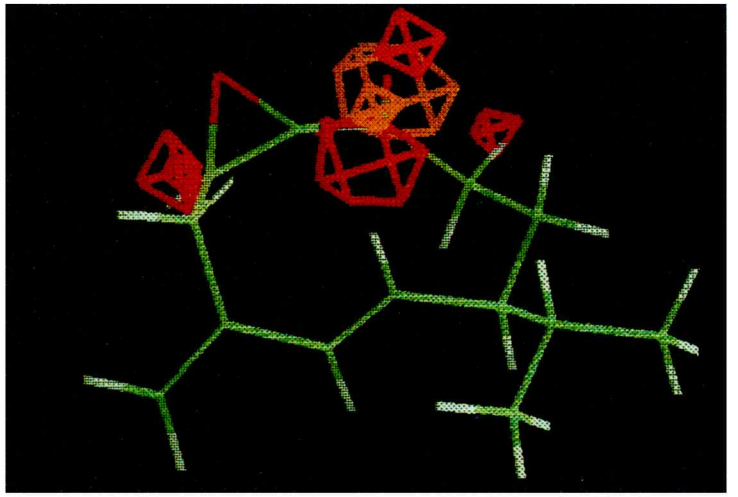

next-LUMO (E = 0.697)

Fig. 13 Frontiér orbital of the global minimum of **3**; the value of each frontier orbital energy (E/eV) is shown in parentheses

Table 7 Population-weighted frontier-orbital energy (eV), $EF^{(N)}$, $EF^{(N)}_{(s)}$, and biological activity of compounds

Compound	HOMO (eV)	$FUMO_{lower}$ [a] (eV)	$FUMO_{upper}$ [b] (eV)	$EF^{(N)}$	$EF^{(N)}_{(s)}$ [c]	Biological activity [d]
1	−9.290	0.386	0.470	4.225	3.634	−13
2	−9.555	1.022	0.511	3.994	3.011	−9
3	−9.330	0.311	0.693	2.792	2.069	−7
4	−9.014	0.522	1.077	1.549	0.789	−6
5	−8.632	0.688	1.261	1.413	0.376	−5

[a] Frontier unoccupied orbital around upper part of ten-membered ring. [b] Frontier unoccupied orbital around lower part of ten-membered ring. [c] Effective frontier parameter. [d] $\log_{10}$[threshold (g)].

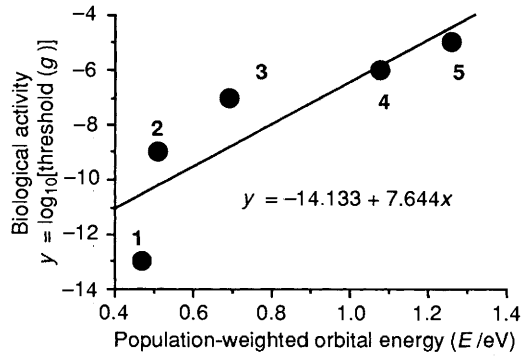

Fig. 14 Relation between biological activity and population-weighted orbital energy of $FUMO_{upper}$ (R = 0.849, σ = 1.93, $t_{statistic}$ = 2.78 and n = 5). The number of compounds shows their activity level.

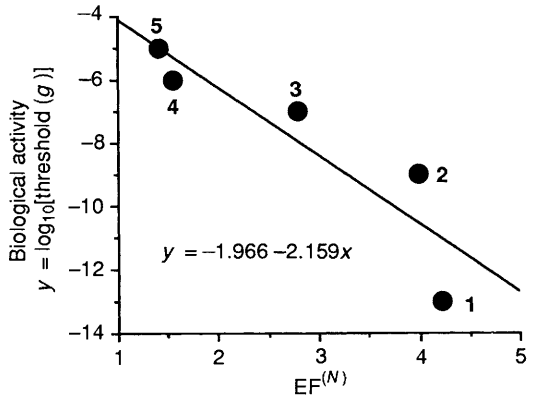

Fig. 15 Relation between biological activity and the value of $EF^{(N)}$ of compounds (R = 0.899, σ = 1.60, $t_{statistic}$ = 3.56 and n = 5)

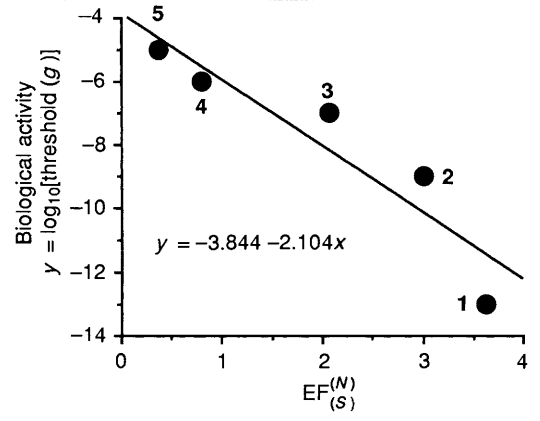

Fig. 16 Relation between biological activity and the value of $EF^{(N)}_{(s)}$ of compounds (R = 0.929, σ = 1.35, $t_{statistic}$ = 4.35 and n = 5)

number of atoms considered, μ is the number of local minima, M is the total number of local minima, $E_{FUMO_{upper}}$ is the frontier orbital energy of $FUMO_{upper}$ (eV), and Pop is the population of each local minimum at 25 °C.

First, the frontier electron density of atom r on $FUMO_{upper}$ is calculated [$f_r^{(N)}$]. Then, $f_r^{(N)}$ is divided by its own orbital energy ($E_{FUMO_{upper}}$), and averaged by the Boltzmann population (Pop) ($Ef_r^{(N)}$). $EF^{(N)}$ is the sum of $Ef_r^{(N)}$ of all non-hydrogen atoms considered. The correlation between the activities and $EF^{(N)}$ of all **1**–**5** compounds was examined. $EF^{(N)}$ is supposed to reflect the population-weighted total contribution of electronic effects. In Fig. 15, biological activity *vs.* $EF^{(N)}$ is plotted. A better correlation (R = 0.899) than that of the plot of biological activity *vs.* population-weighted frontier orbital energy of $FUMO_{upper}$ (Fig. 14). was found.

Next, we calculated the effective frontier parameter $EF^{(N)}_{(s)}$ by taking into account the contribution of the ring structure. The effective frontier parameter $EF^{(N)}_{(s)}$ is hence defined as eqn. (4) where A is the structure factor: 1, the ring conformation is

$$Ef_r^{(N)}{}_{(s)} = \Sigma\{f_r^{(N)}{}_{\mu}/E_{(FUMO_{upper})\mu}\} \times Pop_{\mu} \times A \qquad \mu = 1\text{–}M \quad (4)$$

well superimposable on that of X-ray structure of **1**; 0, the conformation is not superimposable.

$$EF^{(N)}_{(s)} = \Sigma\{Ef_r^{(N)}{}_{(s)}\} \qquad r = 1\text{–}R \quad (5)$$

The effective frontier parameter $EF^{(N)}_{(s)}$ correlates with biological activity (R = 0.929) as shown in Fig. 16. This correlation indicates that the ring conformation, which is found in the global minimum of **1**–**4** and the third most stable conformer of **5**, should be better maintained in order to improve the biological activity. The effective frontier parameter $EF^{(N)}_{(s)}$ may provide some evidence that conformation is important to biological activity and can be used as an index to evaluate pheromone activity.

Conclusion

Detailed structural information of stable conformers of periplanone-B (**1**) and their analogues **2**–**5** obtained by CONFLEX/MM2 are compared. The validity of the calculated results was confirmed by comparison with X-ray crystallographic and NMR results.

The biological activity of **1** and the analogues **2**–**5** can be explained as the combined effect of electronic properties and geometries of stable conformers. In the present case, the unoccupied frontier orbital localized mainly around C9–C10–C1–C2 including carbonyl and spiro-epoxy groups ($FUMO_{upper}$) is important for biological activity. It seems that the proper ring structure and the relative orientation of carbonyl and epoxy groups, which are observed in X-ray studies of **1**, are necessary for biological activity. The newly proposed effective frontier parameter $EF^{(N)}_{(s)}$ takes into account the contribution of all of the stable conformers, and correlates well with biological activity in the series of compounds **1**–**5**. Although related studies [1–6] have been reported, they were concerned only with a few major conformers. In our study, the contributions of all stable conformers are taken into account. This correlation

between the biological activity and effective frontier parameter $EF^{(N)}_{(s)}$ found in this study may provide valuable information for the discussion on the nature of pheromone recognition systems of insects.

References

1 T. Liljefors, B. Thelin, J. N. C. Pers and C. Löfstedt, *J. Chem. Soc., Perkin Trans. 2*, 1985, 1957.
2 A. T. Maynard, L. G. Pedersen, H. S. Posner and J. D. McKinney, *Molecular Pharmacology*, 1986, **29**, 629.
3 M. N. Ramos and B. B. Neto, *J. Comput. Chem.*, 1990, **11**, 569.
4 A. K. Debnath, R. L. L. Compadre, G. Debnath, A. J. Shusterman and C. Hansch, *J. Med. Chem.*, 1991, **34**, 786.
5 B. Waszkowycz, I. H. Hiller, N. Gensmantel and D. W. Payling, *J. Chem. Soc., Perkin Trans. 2*, 1991, 225.
6 M. Froimowitz and S. Rämsby, *J. Med. Chem.*, 1991, **34**, 1707.
7 T. Chuman, K. Shimazaki, M. Mori, K. Okada, H. Gotō, E. Ōsawa, K. Sakakibara and M. Hirota, *J. Chem. Ecol.*, 1990, **16**, 2877.
8 (*a*) K. Shimazaki, M. Mori, K. Okada, T. Chuman, H. Gotō, E. Ōsawa, K. Sakakibara and M. Hirota, *J. Chem. Ecol.*, 1991, **17**, 779; (*b*) H. Gotō, *J. Org. Chem.*, submitted.
9 C. J. Persoons, F. J. Ritter and W. J. Lichtendonk, *Proc. Kon. Ned. Akad. Wetensch. Amsterdam*, 1974, C**77**, 201 (*Chem. Abstr.*, **81**, 88–209f); for a review on American cockroach sex pheromones, see: C. J. Persoons, F. J. Ritter, P. E. J. Verwiel, H. Hauptmann and K. Mori, *Tetrahedron Lett.*, 1990, **31**, 1747, and references cited therein.
10 K. Okada, M. Mori, K. Shimazaki and T. Chuman, *J. Chem. Ecol.*, 1991, **17**, 695.
11 M. Mori, K. Okada, K. Shimazaki and T. Chuman, *Tetrahedron Lett.*, 1990, **31**, 4037.
12 M. Mori, K. Okada, K. Shimazaki, T. Chuman, S. Kuwahara, T. Kitahara and K. Mori, *J. Chem. Soc., Perkin Trans. 1*, 1990, 1769.
13 W. C. Still, *J. Am. Chem. Soc.*, 1979, **101**, 2493.
14 Y. Shizuri, S. Yamaguchi, Y. Terada and S. Yamamura, *Tetrahedron Lett.*, 1987, **28**, 1791.
15 T. Takahashi, Y. Kanda, H. Nemoto, K. Kitamura, J. Tsuji and Y. Fukazawa, *J. Org. Chem.*, 1986, **51**, 3393.
16 T. Takahashi, T. Doi and H. Nemoto, *J. Synth. Org. Chem., Jpn.*, 1989, **47**, 135.
17 H. Hauptmann, G. Mühlbauer and N. P. C. Walker, *Tetrahedron Lett.*, 1986, **27**, 1315.
18 K. Sakakibara, M. Hirota, K. Shimazaki and T. Chuman, *J. Chem. Soc., Perkin Trans. 2*, in preparation.
19 H. Gotō and E. Ōsawa, *J. Am. Chem. Soc.*, 1989, **111**, 8950.
20 (*a*) T. Kitahara, M. Mori, K. Koseki and K. Mori, *Tetrahedron Lett.*, 1986, **27**, 1343; (*b*) T. Kitahara, M. Mori and K. Mori, *Tetrahedron*, 1987, **43**, 2689.
21 U. Burkert and N. L. Allinger, *Molecular Mechanics*, ACS Monograph 177, American Chemical Society, Washington, DC, 1982.
22 (*a*) C. A. G. Haasnoot, F. A. A. M. de Leeuw and C. Altona, *Tetrahedron*, 1980, **36**, 2783; (*b*) S. Masamune, P. Ma, R. E. Moore, T. Fujiyoshi, C. Jaime and E. Ōsawa, *J. Chem. Soc., Chem. Commun.*, 1986, 261.
23 *QCPE* Program No. 506, AMPAC version 2.1.
24 P. T. Beursken, DIRDIF, *Direct Methods for Difference Structures—an Automatic Procedure for Phase Extension and Refinement of Difference Structure Factors*, Technical Report 1984/1, Crystallography Laboratory, Toernooiveld, 6525 ED Nijmegen, Netherlands.
25 C. J. Gilmore, MITHRIL, *An Integrated Direct Methods Computer Program*, University of Glasgow, Scotland; see also *J. Appl. Crystallogr.*, 1984, **17**, 42.

Paper 1/05958K
Received 25*th November* 1991
Accepted 14*th January* 1992